transitions correspond to different trapping sites. This model, when applied to the experimental results for RbMnF₃, and RbMnF₃:Nd³⁺, explains qualitatively the two emission bands of Mn²⁺, the large decrease in energy between manganese absorption and emission, the thermal quenching of the shallower Mn²⁺ emitting center by the exciton absorption band, and the energy transfer Mn²⁺ → Nd³⁺ occuring only through the exciton absorption band.

V. SUMMARY OF RESULTS

The investigation of the absorption, excitation, and fluorescence spectra of Mn²⁺ and Nd³⁺ in RbMnF₃ leads to the following results:

(1) The fluorescence emission of the Mn²⁺ ion is due to two real metastable levels which can be excited only via the Mn²⁺ absorption bands.

(2) The strong thermal quenching of the intensity and lifetime of the 5820 Å bands is due to a thermaliza-tion process between the corresponding level and the short-lived A level of the lowest absorption band.

(3) The decay pattern of the 6300 Å band is explained as due to the action of fast-decay processes from the absorption band and of slower energy-transfer processes from the 5820 Å metastable level.

(4) In the Nd-doped RbMnF₃, the excitation spectra give evidence of Mn → Nd energy transfer even at room temperature. The Mn²⁺ → Nd³⁺ energy-transfer process is of nonradiative type.

(5) The observed changes in the Nd³⁺ fluorescence intensity, decay patterns, and lifetime can be attributed to excitation of neodymium by energy transfer from the manganese-absorption bands and from the 5820 Å manganese level via the lowest Mn²⁺ absorption band.

ACKNOWLEDGMENTS

Electron Paramagnetic Resonance of Gd³⁺ in Zircon Structures. II. YVO₄, YPO₄, YAsO₄

JACK ROSENTHAL* AND REED F. RILEY

The Bayside Laboratory, Research Center of General Telephone & Electronics Laboratories Incorporated, Bayside, New York 11360

AND

U. RANON†

McDonnell Douglas Corporation, Santa Monica, California 90406

(Received 22 August 1968)

The EPR spectrum of Gd³⁺ in the three zircon hosts YVO₄, YPO₄, and YAsO₄ has been analyzed and shown to fit a tetragonal spin Hamiltonian. Crystal-field parameters are given. The technique for determining the absolute sign of the axial parameters is shown.

I. INTRODUCTION

IN previous work[1] on YVO₄, hereafter referred to as I, we initiated a program of EPR investigations of Gd³⁺ in zircon structures. The present research is an extension of this program to include the two additional hosts YPO₄ and YAsO₄, as well as low-temperature measurements on YVO₄. As pointed out in I, most EPR investigations of S-state ions (Gd³⁺ and Eu²⁺ among the rare earths; Mn²⁺ and Fe³⁺ among the transition elements) are motivated by one (or both)

of two concerns: (a) the mechanism for the removal of the ground-state spin degeneracy, and (b) the symmetry and magnitude of the host crystal field. The first is now mostly a theoretical problem because a considerable number of published spectra exist and further proliferation of results is not likely to illuminate the underlying mechanism. The emphasis will shift if any theoretical advance can suggest model systems to test theory. The second of the above concerns dominates at present, and it is our prime concern here. We hope, too, that an examination of systematics in various materials having the zircon structures will help to give some coherence to the crystal-field parameters that have been determined.

We have included a discussion of the method for determining the absolute sign of the axial crystal-field parameters.

[1] J. Rosenthal, Phys. Rev. 164, 363 (1967).

II. CRYSTAL STRUCTURE

The phosphate crystals were grown as described by Brecher et al.,[2] while the $YAsO_4$ crystal growth followed the technique given by Feigelson.[3] The vanadate crystal on which low-temperature measurements were done was obtained from Union Carbide Corporation. The compounds show the tetragonal zircon structure (space group D_{4h}^{19}-14 amd) with unit cell dimensions of $a=7.10$ Å, $c=6.27$ Å for YVO_4,[4] $a=6.878$ Å, $c=6.036$ Å for YPO_4,[5] and $a=7.039$ Å, $c=6.292$ Å for $YAsO_4$.[4] The local site of the Gd ion which enters substitutionally for yttrium has D_{2d} symmetry which is defined by a dodecahedral array of the eight neighboring oxygen ions.

III. THEORY

The relevant theory for this investigation has been given or referenced in I. We summarize here. The $(4f^7)$ $^8S_{7/2}$ ground state in the D_{2d} site is split into four Kramers doublets. Thus we assume a spin Hamiltonian of the form

$$H = g_{||}\beta H_z S_z + g_{\perp}\beta(H_x S_x + H_y S_y)$$
$$+ B_2^0 O_2^0 + B_4^0 O_4^0 + B_6^0 O_6^0 + B_4^4 O_4^4 + B_6^4 O_6^4. \quad (1)$$

The B_n^m are crystal-field parameters (constants) while the O_n^m are the corresponding operators with matrix elements proportional to those of the related spherical harmonics. This form of the spin Hamiltonian implies a spin $S = \frac{7}{2}$ system exposed to a crystal field of tetragonal symmetry.

It is usually more convenient to work with parameters b_n^m rather than the $B_n^m s$. The $b_n^m s$ are given by $b_2^0 = 3B_2^0$, $b_4^m = 60B_4^m$, $b_6^0 = 1260B_6^0$, and $b_6^4 = 60B_6^4$.

IV. EXPERIMENTAL RESULTS

Measurement techniques and the method of analysis of experimental results are basically similar to those described in I. The room-temperature measurements were performed at a microwave frequency of approximately 23.8 GHz and line positions were determined from proton resonance with a precision better than 0.5 G. The low-temperature measurements were done at 10 and 34 GHz. Gd^{3+} in YVO_4, YPO_4, and $YAsO_4$ exhibits a single, seven-line tetragonal spectrum with the fourfold axis along the c axis of the crystal. This, of course, defines the z axis of the spin Hamiltonian (1). In structure, the spectra of these three compounds are identical.

The values of the axial crystal-field parameters b_2^0, b_4^0, and b_6^0 were calculated from the spacings between corresponding lines on either side of the central line,

[2] C. Brecher, H. Samelson, R. Riley, and A. Lempicki, J. Chem. Phys. 49, 3303 (1968).

[3] R. S. Feigelson, J. Am. Ceram. Soc. 50, 433 (1967).

[4] R. W. G. Wyckoff, Crystal Structures (Interscience Publishers, Inc., New York, 1965), 2nd ed., Chap. VIII.

[5] I. Krstanovic, Z. Krist. 121, 315 (1965).

with the static field in the z direction. The technique for determining b_4^4 and b_6^4 from the data along the x axis differed slightly from that used in I. Although useful values of these parameters for the vanadate were obtained from second-order perturbation theory (i.e., useful for starting trial values in an exact diagonalization), the larger value of b_2^0 for YPO_4 weakened the second-order calculation, and an exact diagonalization by computer with trial and error search was employed directly. With the vanadate results at hand, this was not inconvenient. The arsenate results for those parameters were obtained directly from the computer search. Second-order corrections to the axial parameters were found to be negligible. The results are shown in Table I. Although the sign of b_2^0 for the arsenate has not been experimentally verified, there is little reason to doubt its validity. With the values shown in the table, the spectrum along x (or y) was fit to better than 2 G. We did not observe any anisotropy in the g value.

The array of parameters given in Table I is lacking in any obvious pattern that might shed light on the internal fields of the three zircon structures. Certainly, the quality of the fit to the tetragonal Hamiltonian in each case supports the D_{2d} site symmetry. The value of b_2^0 is, in all cases, much larger than the other parameters. This is usually the case for Gd^{3+} and is not characteristic of these particular hosts. There is some persistence of the sixth-order parameters throughout the series, but this may be deceptive in view of the relatively large (fractional) errors in these quantities. Can we deduce anything about the crystal field, other than site symmetry, from these parameters? The near equality of the fourth-order tetragonal parameters (b_4^4) for the YVO_4 and $YAsO_4$ hosts might suggest that they reflect the magnitude of the crystal field when we note the relatively close agreement of the b_2^0 values. However, we must attribute this to coincidence since we fail to find support for any such pattern in the YPO_4 parameters. In addition, any such regularity is obviously not carried through in the values of b_4^0 for the two compounds. If we note that, for all three hosts, the ligands are the same and the lattice constants are quite close, it is fairly certain the the mechanism that determines the spin Hamiltonian parameters for Gd^{3+} cannot be understood in simple crystal-field terms.

V. DETERMINATION OF THE ABSOLUTE SIGN OF b_2^0

The relative sign of all the crystal-field parameters b_n^m is determined once the spectrum is assigned and fit to the spin Hamiltonian. Determination of the absolute sign of the parameters is possible at low temperature when the Boltzmann factor changes appreciably between the various levels of the $S = \frac{7}{2}$ state.

Since b_2^0 is by far the largest crystal-field parameter in the cases presented here, the other parameters will

TABLE I. Spin Hamiltonian parameters for Gd³⁺ in YVO₄, YPO₄, and YAsO₄. All $b_n{}^m$'s in units of 10^4 cm⁻¹.
Signs for YAsO₄ are relative. Values for YVO₄, 300°K are from the work of Rosenthal.[a]

| | YVO₄ | | YPO₄ | | YAsO₄ |
	300°K	4.2°K	300°K	4.2°K	300°K
$g_{\parallel}$	1.9915±0.0002	1.991±0.001	1.9915±0.0002	1.991±0.001	1.9917±0.0002
$g_{\perp}$	1.9915±0.0002	1.991±0.001	1.9915±0.0002	1.991±0.001	1.9917±0.0002
$b_2{}^0$	−441.6 ±0.2	−480 ±1.0	−727.9 ±0.1	−742.3 ±0.6	(−)316.5 ±0.2
$b_4{}^0$	−1.5 ±0.1	−1.6 ±0.2	−4.1 ±0.1	−4.15 ±0.06	−4.2 ±0.1
$b_6{}^0$	0.8 ±0.6	0.46 ±0.1	0.4 ±0.1	0.49 ±0.05	0.4 ±0.5
$b_4{}^4$	41.5 ±0.4	34 ±1	21.2 ±0.4	22.8 ±0.5	43.5 ±0.2
$b_6{}^4$	0.0 ±0.2	0.16 ±0.14	0.0 ±0.2	0.0 ±0.5	0.0 ±0.2

[a] Reference 1.

be neglected in the following discussion. Applying the external magnetic field parallel to the z axis and neglecting hyperfine terms, the spin Hamiltonian is

$$H = g_{\parallel}\beta H S_z + b_2{}^0[S_z{}^2 - \tfrac{1}{3}S(S+1)].\qquad (2)$$

For S-state ions $g_{\parallel}$ is close to the free-electron g value and is thus positive. This means that for any field H, the state with $-S_z$ will be of lower energy than the state with $+S_z$. The energy levels of (2) are plotted in Figs. 1 and 2 for the case of YVO₄ with $b_2{}^0 > 0$ and $b_2{}^0 < 0$, respectively. The X-band transitions are also indicated in these figures. The energy levels of (2) are simply

$$E(M) = GM + b_2{}^0(M^2 - 21/4),\qquad (3)$$

where $G = g_{\parallel}\beta H$. The $M \rightarrow M+1$ transitions are given by

$$G_0 = G + (2M+1)b_2{}^0,\qquad (4)$$

where $G_0 = h\nu$ and ν is the microwave frequency. The relative intensity of such a transition is given by

$$[63/4 - M(M+1)]\exp(-\Delta E/kT),\qquad (5)$$

where the exponent is the Boltzmann factor. The first term in (5) gives the familiar 7:12:15:16:15:12:7 intensity distribution for the $S = \tfrac{7}{2}$ spectrum in an axial field at room temperature. These intensities may be modified considerably at liquid-helium temperatures by the Boltzmann factor. From Figs. 1 and 2 it is seen that with $b_2{}^0 > 0$ the Boltzmann factor is 1 for the high-field transition, independent of the field, and is less than 1 for the other transitions. In this case, therefore, the intensity of the low-field lines is slightly reduced relative to the high-field lines when the spectrum is observed at liquid-helium temperature. On the other hand, with $b_2{}^0 < 0$, the Boltzmann factor decreases with the field and a sharp decline is expected in the intensities of the high-field lines. The two quite different spectra
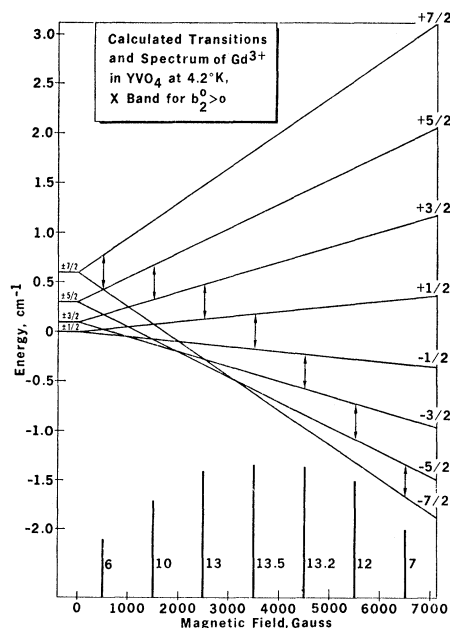

FIG. 1. Calculated energy levels and spectrum for YVO₄:Gd³⁺ at X band, 4.2°K along the z axis for $b_2{}^0 > 0$.
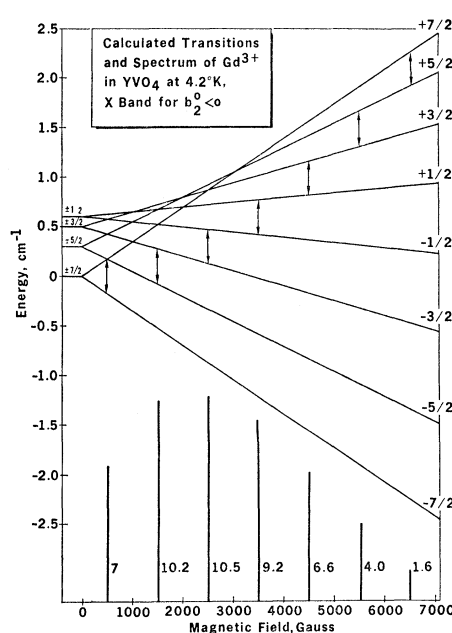

FIG. 2. Calculated energy levels and spectrum for YVO₄:Gd³⁺ at X band, 4.2°K along the z axis for $b_2{}^0 < 0$.
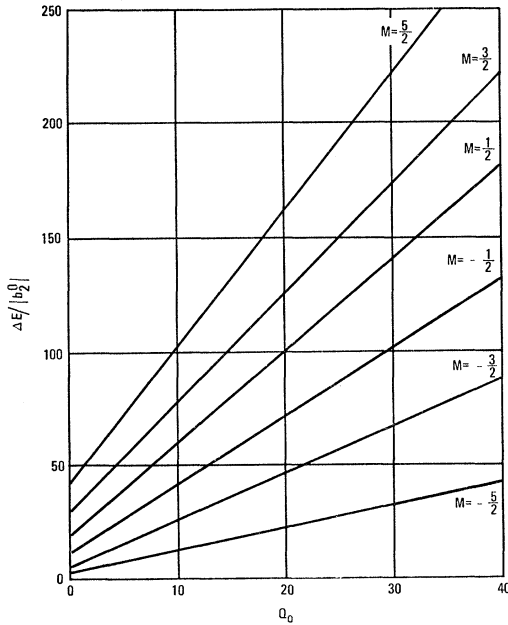
FIG. 3. Energies of Zeeman levels of $S=\frac{7}{2}$ state in an axial field, for $\mathbf{H}\|z$, as a function of the microwave quantum energy; both scales normalized to b_2^0.

expected for $b_2^0>0$ and $b_2^0<0$ are shown in Figs. 1 and 2. By comparison with the experimental spectrum it is easy to determine the sign of b_2^0.

From (3) and (4) we compute ΔE in terms of b_2^0 and the microwave quantum energy G_0 for the case $b_2^0<0$.

$$-\Delta E = E(-\tfrac{7}{2}) - E(M)$$
$$= -[(\tfrac{7}{2}+M)G - (M^2+7/4)|b_2^0|]$$
$$= -[(\tfrac{7}{2}+M)G_0 + (M^2+8M+63/4)|b_2^0|]. \quad (6)$$

It is convenient to express the energy difference in units of b_2^0; therefore, we define $G_0/|b_2^0| = Q_0$. The energies of the Zeeman levels in terms of Q_0 are given in Table II. These energy differences are plotted in Fig. 3 as a function of Q_0. The parameters b_2^0 and H_0 are frequently given in cm^{-1} or GHz. It is useful, therefore, to have the Boltzmann constant k in these units too so that the Boltzmann factor can be computed from the known temperature and from ΔE given in

TABLE II. Normalized energies of Zeeman levels of a $S=\frac{7}{2}$ state in a b_2^0 crystal field for $\mathbf{H}\|z$.

M	$\frac{5}{2}$	$\frac{3}{2}$	$\frac{1}{2}$	$-\frac{1}{2}$	$-\frac{3}{2}$	$-\frac{5}{2}$
$\Delta E/|b_2^0|$	$6Q_0+42$	$5Q_0+30$	$4Q_0+20$	$3Q_0+12$	$2Q_0+6$	Q_0+2

Fig. 3:

$k = 1.381 \times 10^{-16}$ erg/$^\circ$K $= 0.695$ cm^{-1}/$^\circ$K
$$= 20.85 \text{ GHz}/^\circ\text{K}.$$

As an example we compute the relative intensities of the Gd^{3+} lines in YPO$_4$ at X band and Ka band (0.3 and 1.2 cm^{-1}, respectively) at both 1.8 and 4.2°K. From Table I, $b_2^0 = 0.073$ cm^{-1}, so that $Q_0 = 4.1$ at X band and $Q_0 = 16.5$ at Ka band. From Fig. 3 the energy differences $\Delta E/|b_2^0|$ are X band: 6, 14, 24, 36, 50, and 66; Ka band: 18, 38, 59, 83, 110, and 138. At 1.8°K, $kT = 17.1|b_2^0|$ and at 4.2°K, $kT = 40|b_2^0|$. From these data the Boltzmann factors are easily computed and from (5) the relative intensities are then obtained. These are shown in Table III.

Data such as in Table III are useful only for comparing intensities at a given microwave frequency (assuming that the same microwave power is used at the different temperatures). Changing the microwave frequency involves changes in the cavity filling factor, in the microwave field in the cavity, and often also in

TABLE III. Relative intensities of YPO$_4$:Gd^{3+} lines at X and Ka bands; 1.8 and 4.2°K.

	M	$-\frac{7}{2}$	$-\frac{5}{2}$	$-\frac{3}{2}$	$-\frac{1}{2}$	$\frac{1}{2}$	$\frac{3}{2}$	$\frac{5}{2}$
X	1.8°K	7	8.4	6.6	3.9	1.8	0.6	0.14
band	4.2°K	7	10.3	10.5	8.8	6.1	3.5	1.3
Ka	1.8°K	7	4.2	1.6	0.5	0.1	0.02	0.002
band	4.2°K	7	7.7	5.9	3.5	1.8	0.7	0.2

sample size. All these will change the absolute intensity of the transitions.

From this example it can be seen that there is no point in going to 1.8°K for measurement of crystal-field parameters in this case since some of the lines may not be seen at all.

Note added in proof. The determination of the crystal-field parameters of Gd^{+3} in YVO$_4$ and YPO$_4$ from variable-frequency EPR has just been reported by W. Urban, J. Chem. Phys. **49**, 2703 (1968). The results are in good agreement with those given here.

ACKNOWLEDGMENTS